

Tuning the nature of nitrogen atoms in N-containing reduced graphene oxide

Stefania Sandoval^a, Nitesh Kumar^b, Judith Oro-Solé^a, A. Sundaresan^b, C. N. R. Rao^{b,*}, Amparo Fuertes^a, and Gerard Tobias^{a,*}

^a Institut de Ciència de Materials de Barcelona (ICMAB-CSIC), Campus de la UAB, 08193 Bellaterra (Barcelona), Spain.

^b International Centre for Materials Science, Chemistry and Physics of Materials Unit, New Chemistry Unit and CSIR Centre of Excellence in Chemistry, Jawaharlal Nehru Centre for Advanced Scientific Research (JNCASR), Jakkur P.O., Bangalore – 560064, India.

Physical and chemical properties of graphene can be tailored by nitrogen doping. As a consequence of the continuous race to achieve the highest possible amount of doping there is a growing tendency to assume that all N species are incorporated within the graphene lattice (doping). Here we show that this is not always the case and employ several complementary techniques that allow a proper assessment of the type of nitrogen present. The nature of the nitrogen atoms has been tuned by ammonolysis of graphene oxide in the range of 100 °C-800 °C. This allows us to expand the capabilities of the synthetic approach to afford not only N-doping (at high temperature) but also to introduce amine and amide moieties at 100 °C; the latter presenting a much higher dispersability in aqueous media than graphene oxide. Interestingly, the sample with the highest amount of nitrogen (14.7 wt. %) cannot be referred to as N-doped graphene since it also contains N-bearing aliphatic moieties.

*Corresponding authors. E-mail: gerard.tobias@icmab.es (Gerard Tobias); cnrrao@jncasr.ac.in (C.N.R.Rao).

1. Introduction

Graphene, the main building block of all graphitic materials (which include carbon nanotubes and fullerenes), has recently attracted a great interest due its promising applications in important fields such as batteries, sensors, and biomedicine.[1] Its structure, a monolayer of sp^2 hybridized carbon atoms packed into a 2-D honeycomb lattice, confers it extraordinary physical, electrical and mechanical properties, including high electrical mobility, chemical and thermal stability and high surface area.[2, 3] Many approaches have been explored to tune these properties and further expand the range of applications. Chemical functionalization and doping are an efficient way to tailor the physical and chemical behaviour of materials.[4, 5] In this context, N-doping is an interesting approach since this not only allows n-type doping[6] and improves its performance in electrocatalysis,[7, 8] supercapacitors,[9] sensors[10] or as magnetic material,[11, 12] but also confers enhanced thermal stability;[13] thus extending its potential in fuel cell applications and other fields where high temperatures are required.[4, 14, 15] Different methods have been explored to introduce nitrogen either (i) during the synthesis of the graphene sheets via chemical vapour deposition (CVD)[16] and arc discharge,[17] or (ii) via a post synthesis modifications. The majority of post synthesis doping strategies usually employ graphene oxide (GO) as starting material. GO has been doped in the presence of ammonia at high temperature,[18] by means of plasma treatment,[19] and under hydrothermal conditions with aqueous ammonia [20] and hydrazine.[21] The latest has been extensively employed for the preparation of reduced graphene oxide (RGO), however in terms of doping the hydrazine approach does not exceeds ca. 5 % of nitrogen. The amount of nitrogen and level of reduction achieved by each particular method determines the electrical and conducting properties of the resulting material,[6] depending not only on the chosen technique but also on the experimental conditions employed. In the continuous race to achieve the highest possible amount of N-doping,[22] the nature of the resulting N atoms is sometimes overlooked. X-ray photoelectron spectroscopy (XPS) is the most widely employed technique to characterize the resulting materials. Despite XPS provides information on the N environment but cannot unambiguously discern between N-bearing aliphatic functionalities and N-doping.[23] Therefore there is a growing tendency to assume that all N species are incorporated within the graphene lattice (doping). In this article, we show that this is not always the case and employ several complementary techniques that allow a proper assessment of the type of nitrogen present. These include not only XPS, FTIR and UV-Vis spectroscopies that are the most commonly employed methods for the determination of functional groups, but also benefit from other techniques that are not typically used for this purpose: thermogravimetric analysis, contact angle measurements and the degree of dispersability. Furthermore, employing gas phase reaction of graphene oxide and ammonia we are able to prepare N-doped reduced graphene oxide at 500 °C and highly dispersable graphene oxide functionalized with amine and amide species under mild conditions (100 °C).

2. Experimental

2.1. Synthesis of graphene oxide (GO): Graphene oxide was synthesized by a modified Hummer's method.[13] Concentrated H_2SO_4 (115 mL) and $NaNO_3$ (2.5 g) were added slowly to graphite powder (5g) ($< 20 \mu m$, Sigma-Aldrich), and the mixture was cooled down to 0 °C. After 30 min, $KMnO_4$ was added slowly (15 g) in order to keep the temperature below 20 °C. The reaction was warmed to 35 °C and stirred for 30 min. Afterwards, the mixture was cooled to room temperature and 230 mL of water were added slowly maintaining the reaction temperature at 98 °C for 2 h. Then, additional water (1 L) and 30% H_2O_2 solution (5 mL) were added slowly. The content was air cooled and purified washing with distilled water followed by centrifugation until the pH of the solution was neutral.

2.2. Synthesis of nitrogen functionalized RGO and nitrogen doped RGO: GO was annealed in the presence of pure ammonia gas (Carbueros Metálicos 99.99%) with a flow rate of 300 mLmin⁻¹ and 1 h of treatment. In order to study the effect of the treatment temperature in the simultaneous reduction and doping of graphene oxide, samples were heated at temperatures ranged between 100 °C and 800 °C. For each synthesis 100 mg of GO were spread into a sintered Al₂O₃ boat and placed into a silica furnace tube.

2.3. Characterization: Elemental analyses data were recorded on a Thermo Scientific™ FLASH 2000 Series CHNS Analyzer using a Metler Toledo MX5 microbalance. The morphology of the sheets was studied recording TEM, HRTEM images and SAED patterns. TEM images and SAED patterns were obtained using a JEOL 1210 microscope, operating at 120 kV. HRTEM was carried out in a FEI, Tecnai microscope operating at 200 kV. Samples were prepared sonicating and dispersing in hexane. Afterwards, they were placed dropwise onto a lacey carbon support grid. Thermogravimetric analyses were performed on a Netzsch instrument, model STA 449 F1 Jupiter®, under flowing air at a heating rate of 10 °Cmin⁻¹. For AFM measurements, an INOVA Bruker in tapping mode was used. The sample was sonicated in 1:1 ethanol:water mixture, followed by centrifugation at 5000 rpm. A very diluted dispersion was obtained, which was subsequently dropcast on a cleaned Si substrate. Surface wettability measurements were carried out in a DSA100 Contact Angle Measuring System (Krüss) by the sessile drop method. Contact angle measurements were taken after 5 µL of water were directly dropped into a compact and dried layer prepared after sonication of 5 mg of the sample in 5 mL of water subsequently deposited by vacuum filtration onto a 0.2 µm polycarbonate membrane. After drying, the membrane containing the solid sample was stucked to a glass slide with double-sided tape. FI-IR spectra were recorded in transmission mode on a Perkin-Elmer Spectrum One with an energy range of 450-4000 cm⁻¹. The samples were prepared by dropping 2-propanol dispersions (ca. 10 mg/mL) onto a preheated ZnSe disks (2 mm thickness, 70 °C).[24] For UV-Vis measurements a Varian Cary 5 spectrophotometer with an operational range of 200-nm was used. Samples were prepared by sonication of 1 mg of solid in 5 mL of a 1:1 ethanol:water mixture. Afterwards, the dispersions were centrifuged at 4500 rpm during 15 min. Analyses were carried out in absorbance mode using 1 cm quartz cuvettes, and dispersions were analyzed before and after centrifugation. XPS were recorded in a Kratos AXIS ultra DLD spectrometer using monochromatic Al Kα. All samples were introduced in the preparation chamber as received and on the same substrate (Cu) to maintain the analysis conditions invariable. High resolution spectra of C1s, O1s and N1s regions were also registered. Finally, Raman spectra were recorded using a Horiba Jobin Yvon operating at 532 nm and using 100× objective. Acquisition time was set to 30 s and laser power to 0.5 mW. Spectra were recorded from different spots of the samples prepared by dropping 2-propanol dispersions onto preheated microscope slides.

3. Results and Discussion

Nitrogen-containing reduced graphene oxide samples¹ [25] were synthesized by thermal annealing of GO under a continuous flow of pure ammonia gas at temperatures ranged between 100 °C and 800 °C. Significant ammonia decomposition begins at ca. 500 °C, being important at 700 °C (e.g. above 40 % for a flow rate of 60 mL min⁻¹).[26] As previously reported, both the treatment time and NH₃ flow rate do not play a significant role in the final

¹ Following the nomenclature proposed by Bianco et al.,[25] reduced graphene oxide refers to samples of graphene oxide that have been processed to reduce its oxygen content. This definition includes both, N-doping and substitution of oxygen-moieties by nitrogen. Therefore to discern between structural nitrogen doping and N-aliphatic groups we will refer to the samples as N-doped RGO and N-functionalized RGO respectively.

N content of the samples.[13] Therefore, in the present study these parameters are kept constant for all the treatments (1 h, 300 mL min⁻¹). Figure 1 summarizes the N content of the prepared samples, as determined by elemental analyses. There is no linear correlation between the temperature of treatment and the amount of nitrogen introduced in the samples. An initial increase in the N content is observed reaching its maximum for the sample of GO treated under ammonia at 220 °C (14.7 wt. % of N). Afterwards, a continuous decrease is observed when increasing the temperature of treatment up to 800 °C (7.7 wt. %). For comparison, data on a sample of previously reduced GO (RGO) subsequently treated with ammonia at 500 °C is also included (empty rhombus). The employed RGO was prepared by annealing GO at 1050 °C under Ar/H₂ atmosphere.[13] Elemental analysis confirms the absence of nitrogen in the ammonia treated RGO (Table S1), stressing the importance of having oxygen-bearing functionalities for an efficient ammonolysis treatment.

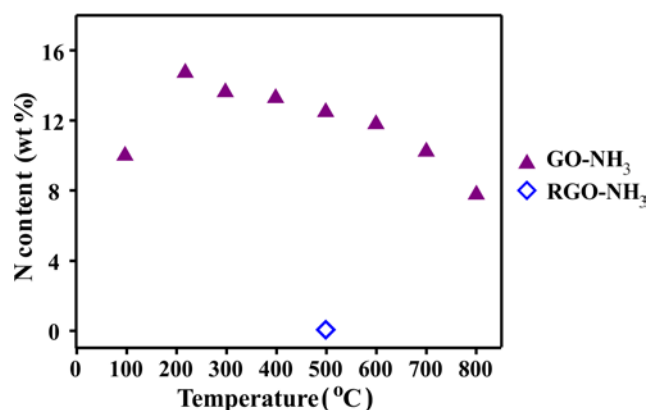


Figure 1. Effect of temperature on the total amount of nitrogen in ammonia treated GO (solid triangles). For comparison a sample of RGO treated in ammonia is also included (empty rhombus).

A transmission electron microscopy (TEM) image of the starting GO is shown in Figure 2(a). The selected area electron diffraction (SAED) pattern (b) shows well defined diffraction spots, confirming the graphitic crystalline structure of the synthesized material, which corresponds to the (100) and (110) planes (d-spacing = 2.12 Å and 1.23 Å) respectively.[27] The higher intensity observed for the inner diffraction spots (twice the intensity of the outer ones) is in agreement with the presence of single-layered graphene oxide. [27] TEM inspection of GO and NH₃ treated samples do not show any apparent change in the morphology of the sheets after the treatment in ammonia. An atomic force microscopy (AFM) image of reduced graphene oxide prepared at 500 °C under NH₃ is presented in Figure 2(c)). Taking into account that single-layered graphene has been reported to have a height of 0.661 nm by AFM,[20] and that the distance between two consecutive layers in graphite is 0.34 nm, the 2.4 nm height recorded in the sample would correspond to about 5 layers. A similar number of layers is observed on the edge of a graphene flake by high-resolution TEM (Figure 2(e)).

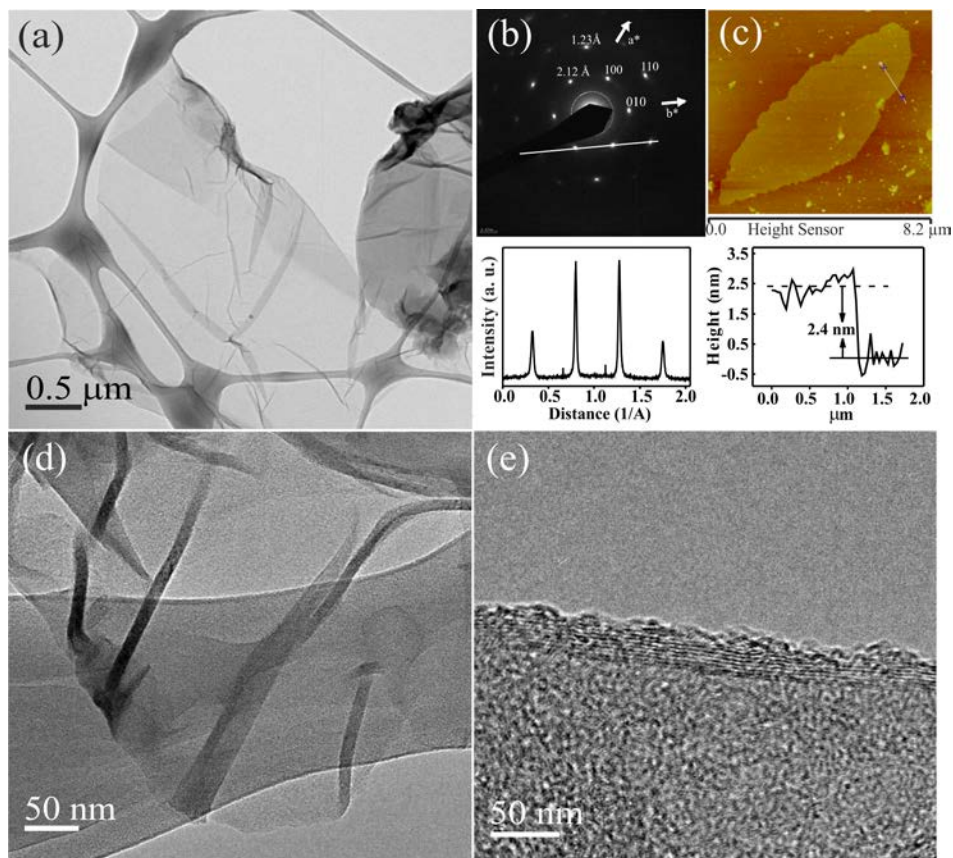


Figure 2. (a) Transmission electron microscopy image and (b) SAED pattern of graphene oxide with the corresponding line profile. (c) Atomic force microscopy and (d,e) TEM of a N-containing reduced graphene oxide sample (prepared at 500 °C).

In order to identify the nature of the different functionalities present in both, GO and the ammonia treated samples, FT-IR spectroscopy was initially carried out. Figure 3 shows the recorded spectra for the lowest (100 °C) and highest (800 °C) temperatures employed, the sample containing the highest amount of N (220 °C) and an additional intermediate treatment (600 °C). GO spectrum (black line) shows the characteristic bands present in oxidized derivatives of graphite,[28, 29] illustrating the presence of free O-H groups ($\nu_{\text{O-H}}$ 3000-3700 cm^{-1}) which can arise from either absorbed water or from the stretching vibrations of phenol and hydroxyl groups when carboxylate moieties (C=O band at $\nu_{\text{C=O}}$ 1723 cm^{-1}) are present. Additionally, the C=C ($\nu_{\text{C=C}}$ 1585 cm^{-1} , from the conjugated structure), C-O stretching ($\nu_{\text{C-O}}$ 1220 cm^{-1}) and O-H bending ($\nu_{\text{O-H}}$ 1120 cm^{-1}) signals, originated by hydroxyl groups closely linked to the structure are also present.[30] Significant changes in the intensity and position of the bands are evident after the ammonolysis treatment. There is a decrease in both, free and linked O-H signals, upon increasing the treatment temperature. Moreover, following the same trend, there is a decrease in the C=O/C=C intensity ratio. The elimination of C=O containing moieties becomes evident already at 600 °C indicating the restoration of the conjugated structure. A new band around 1074 cm^{-1} appears in the low temperature treated samples (100 °C and 220 °C) corresponding to C-N stretching of aliphatic amines. Taking into account that the carbonyl band ($\nu_{\text{C=O}}$ 1723 cm^{-1}) is still clearly visible in both of these samples, the presence of amide groups cannot be disregarded. The C-N band becomes weaker when increasing the treatment temperature suggesting that the N atoms are no longer part of aliphatic functionalities but rather incorporated within the graphene lattice. On the other hand, a triplet at ca. 2900 cm^{-1} is clearly visible in the FT-IR spectra of GO and in the samples treated at 100 °C and 220 °C. Bands in this area can either correspond to an spectral

artefact,[31] or originate from C-H stretching vibrations. In the present study, a decrease of signal intensity is observed for samples treated at high temperatures, in agreement with the amount of hydrogen determined by elemental analyses (2 wt. % in GO; 2.4 wt. % at 100 °C; 1.4 wt. % at 220 °C; 0.4 wt. % at 600 °C and 800 °C; see Table S1). Therefore the band at ca. 2900 cm^{-1} is attributed to C-H bonds, easily correlated to the presence of oxygen and N bearing functionalities in GO and the low temperature ammonia treated samples.

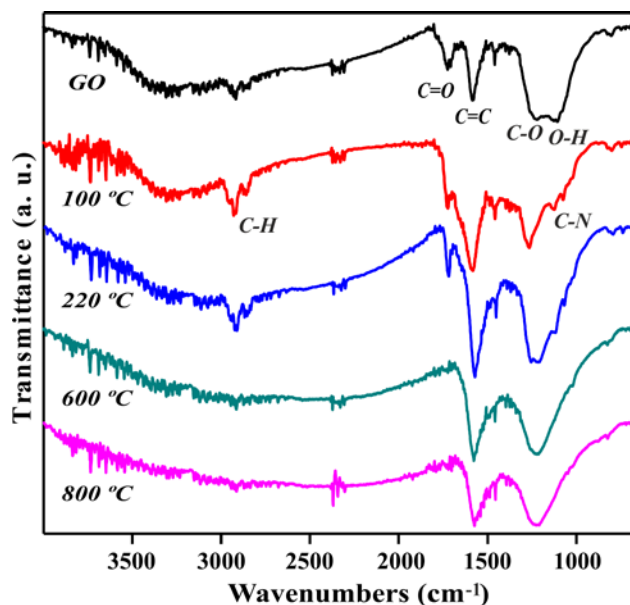


Figure 3. FT-IR of GO and ammonia treated GO at temperatures ranged between 100 °C and 800 °C.

Thermogravimetric analyses (TGA) were next performed to assess the role of the functional groups detected by FT-IR with the thermal oxidation behaviour of the samples. GO has an initial continuous weight loss corresponding to absorbed atmospheric species; typically water, until ca. 200 °C (continuous black line, Figure 4(a)). This is already an indication of the hydrophilicity of the sample, and is also visible for the ammonia treated GO at 100 °C. At 220 °C a remarkable weight loss of 36 % can be observed for GO indicating the elimination of oxygen bearing functionalities. This temperature was therefore selected for subsequent experiments under ammonia, rather than 200 °C, as already presented in Figure 1. The complete combustion of the GO sample takes place at 492 °C. In case of the ammonia-treated samples in the range of 100 °C - 400 °C (dashed lines), events taking place at low temperatures are assigned to the oxidation of both O and N bearing aliphatic functional groups. A progressive decrease in the amount of aliphatic functionalities is clearly visible when increasing the treatment temperature, in agreement with the FT-IR analysis. Additionally, a significant increase in the temperature onset of the complete combustion is observed until 569 °C (for the sample prepared at 400 °C). This behaviour is attributed to the continuous removal of oxygen bearing functionalities, defects, from the structure of GO. However, despite that a significant amount of aliphatic groups have been removed at 400 °C, the presence of these species cannot be discarded. Therefore, this set of samples (100 °C - 400 °C) containing different degrees of aliphatic nitrogen will be referred to as N-functionalized RGO in this study.

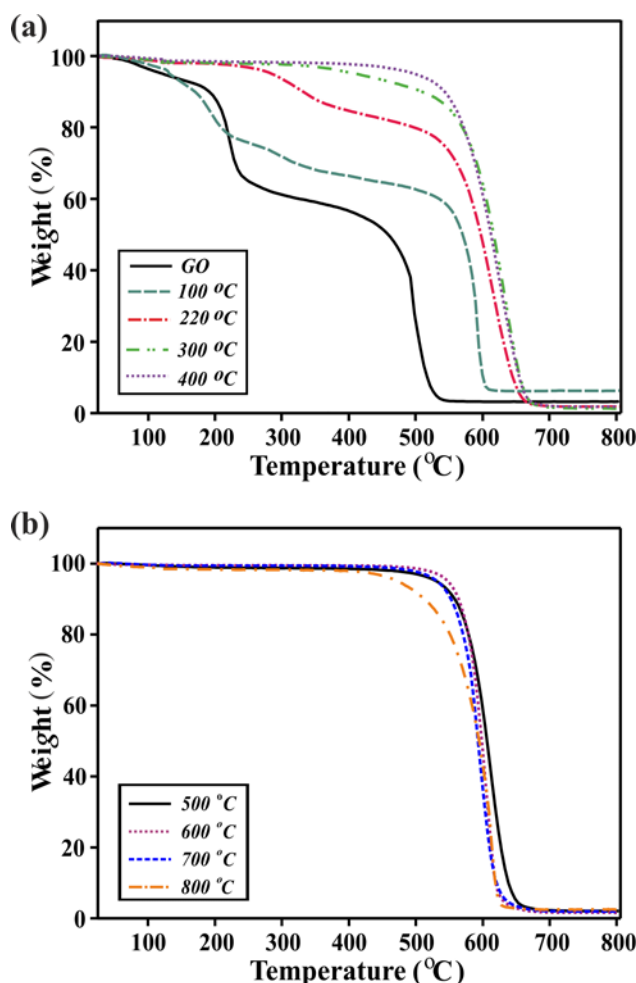


Figure 4. Thermogravimetric analyses of GO and ammonia treated GO at temperatures ranged between (a) 100 °C - 400 °C (low temperature treatments, N-functionalized RGO) and (b) 500 °C - 800 °C (high temperature treatments, N-doped RGO). TGA was performed under flowing air at a heating rate of 10 °C min⁻¹.

Ammonia has been shown to be an efficient reducing agent for the synthesis of RGO, being more efficient at high temperature. When GO is treated above 500 °C in ammonia (Figure 4 (b)) only the process corresponding to the complete combustion of the sample is present by TGA in air. The initial weight loss attributed to oxygen and nitrogen bearing aliphatic functionalities, for the low temperature treated samples, has vanished. This suggests the incorporation of N into the planar structure. Therefore, to differentiate this set of samples prepared at high temperature (500 °C-800 °C) from the low temperature treatments (100 °C-400 °C), the former will be referred as N-doped RGO and the latter, as already mentioned, as N-functionalized RGO. The terminology N-functionalized RGO is employed to stress the presence of aliphatic nitrogen containing moieties in the samples, which tends to be neglected, but N-doping might already have taken place below 500 °C. Furthermore, the samples treated between 500 °C and 800 °C present an inverse trend in thermal stability against oxidation. The higher the N content is, the higher onset of combustion temperature is observed (Table 1).

Table 1. Onset of combustion temperature in air of GO annealed in ammonia at temperatures ranged between 500 °C and 800 °C.

T treatment	N content (wt.%)	Onset of combustion
500°C	12.5	579 °C
600°C	11.8	577 °C
700°C	10.2	571 °C
800°C	7.7	520 °C

For instance, whereas the sample of N-doped RGO prepared at 500 °C, with 12.5 wt.% N, presents an onset of combustion at 579 °C, the sample prepared at 800 °C, with 7.7 wt.% N, starts to oxidize at lower temperatures (520 °C). This behaviour can be understood from a thermodynamic point of view because a graphene fragment leads to a higher release of energy than a fragment of N-doped RGO.[13] One must take into account the enthalpy change involved in breaking the carbon-carbon, carbon-nitrogen and oxygen-oxygen bonds in a combustion reaction and the subsequent formation of the oxidation products (CO₂ and N₂; as per Atkins et al.[32]). The calculated Gibbs energies predict a more spontaneous reaction for the oxidation of undoped graphene compared to the doped samples, in good agreement with the present thermal stability analysis.

As mentioned, the initial loss in TGA observed in GO, also visible for the sample prepared at 100 °C, is typically attributed to desorption of physisorbed molecules. Therefore is an indication of the hydrophilicity of the materials, directly related to the presence of functional groups in carbon nanomaterials.[33] We decided to take advantage of this phenomenon and quantitatively determine the wettability properties by measuring the contact angle of a water droplet lying on a thin layer of the samples. The contact angle measurements of the N-containing RGO samples along with those of GO and graphite are presented in Figure 5. As expected, graphite powder shows the lowest interaction with the droplet, i.e. highest hydrophobicity, of all the analyzed samples due to the absence of functional groups in the structure (contact angle 160.6°) nearly followed by the N-doped RGO samples. In contrast, the N-functionlized RGO samples (100 °C-400 °C) present a more hydrophilic character. As expected, the most hydrophilic of the studied materials is GO (75.0°), followed by the sample prepared at 100 °C. Then a continuous increase of the contact angle is observed upon increasing the temperature of treatment. The observed trend is in agreement with the gradual disappearance of functionalities observed by both FT-IR and TGA when increasing the treatment temperature. The higher wettability of the N-containing samples compared to that of graphite arises from electrostatic interactions of different functional groups with the droplet. In the case of the N-doped RGO samples, small differences are observed with respect to graphite that can originate from the in-plane polarization induced by the presence of N heteroatoms or from thermally stable oxygen functionalities, as reported by Romanos et al.[34] Thus, wettability measurements are a useful and simple tool to provide, in a fast and qualitative manner, information on the degree and type of functionalization of the samples.

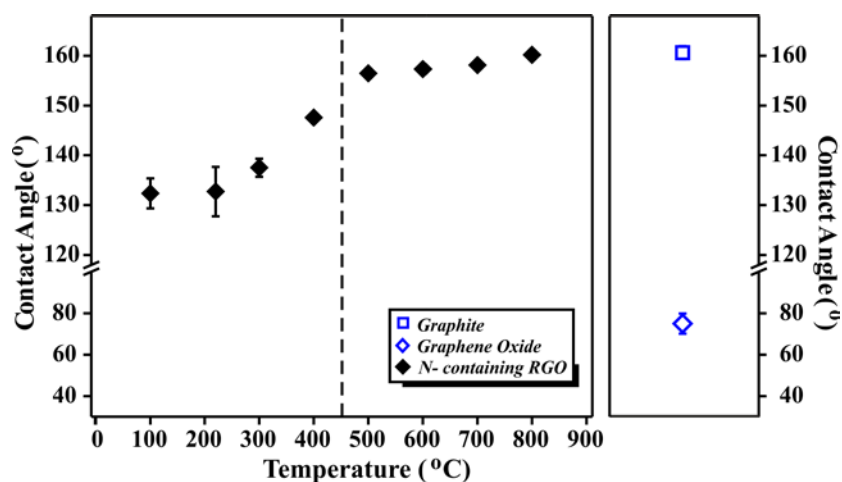


Figure 5. Effect of the temperature of treatment in the wettability of thin layers of the N-containing RGO samples (black solid rhombus), prepared after ammonolysis reactions. Both, graphene oxide (blue empty rhombus) and graphite (blue empty square) are include as benchmarks. The dashed line separates the N-functionalized RGO (100-400 °C) from the N-doped RGO samples (500-800 °C). Error bars are included for all the samples (some of them are almost not visible due to the low error of the measurement).

The hydrophilic character of the samples can also be assessed by the dispersability of the material in aqueous solvents. Figure 6 displays the UV-Vis absorption spectra of GO, and NH_3 treated GO dispersions prepared by sonication (a) and sonication-centrifugation (b) of 1 mg of sample in 5 mL of an ethanol-water (1:1) mixture. There are two well differentiated regions of absorbance in GO (continuous black line), corresponding to the π - π^* (239 nm) and n - π^* (ca. 300 nm) transitions previously assigned to C=C and C=O bonds respectively.[35] The second region of absorbance (shoulder) decreases in the ammonia treated samples until its total disappearance in N-doped RGO samples (see spectra at 500 °C), due to the continuous elimination of oxygen bearing functionalities.[36] Furthermore, a marked shift is observed in the first region (239 nm) when GO spectrum is compared to those of N containing samples (dashed lines). Despite the fact that this shift can be attributed to the gradual restoring of the electronic conjugation, the presence of N atoms in the structure might play a role. Let us focus on the inset of Figure 6 (a). Comparison of the UV-Vis spectrum of the 600 °C NH_3 sample (continuous black line, 10.0 at. % N as per XPS) and the 700 °C sample (blue dotted line, 7.7 at. % N) reveals a major shift to the red area of the spectrum (+7.2 nm). Both samples having similar amounts of oxygen (ca. 2 at. %; Table 2), the origin of the shift must reside in the different N content of the samples. Therefore, the amount of N and its distribution into the layer has a noticeable influence in the spectroscopic properties of the material.[37] The higher the N content and the temperature of treatment is, the higher shift to the red region of the spectra is observed, once taken into account the contribution from the oxygen.

Figure 6 (b) shows UV-vis spectra of the dispersions after centrifugation. There is a marked difference in both the shape and the absorbance between GO and the samples prepared at different temperatures under NH_3 . Both GO and the samples prepared between 100 °C – 300 °C show a good dispersability in water:ethanol due to the presence of oxygen bearing (in the case of GO) and oxygen/nitrogen bearing moieties in N-functionalized RGO, in agreement with FT-IR analysis. The presence of such functional groups enhances the dispersability via the formation of electrostatic interactions between the graphene sheets and the polar solvent. Despite the fact that the solubility of GO would a priori be expected to be higher than the N-

containing samples, an inverse trend is observed for the sample prepared at 100 °C. The formation of intralayer hydrogen bonds in the sample of GO might account for this. Hydroxyl and carbonyl group derivatives, such as quinones, can interact forming internal hydrogen bonds (see Scheme S1).[38] In agreement with previous reports,[35] carbonyl functionalities are found to be the most abundant moieties present in GO (24.0 at. % as determined by XPS, in front of 2.9 at. % of hydroxyl groups; Table 2). The presence of carboxylic groups (3.9 at. %) might also contribute to this fact, through the formation of dimeric moieties resulting from electrostatic interactions. A marked decrease in the amount of C=O (ca. 60%) is observed by ammonolysis of GO at 100 °C. An important decrease in water dispersability is already observed at 400 °C reflecting the continuous elimination of the aliphatic functionalities when increasing the temperature of the treatment.

The inset in Figure 6 (b) presents a picture of the prepared dispersions. To better appreciate the different behaviour of the samples the picture has been taken after a partial centrifugation of the materials. N-functionalized RGO samples treated at 100 °C and 220 °C become darker than GO (brownish) and stable dispersions are obtained. In contrast, a clearer appearance along with the formation of a black precipitate is observed for the high temperature treated samples (500 °C-800 °C) in agreement with the higher hydrophobicity presented by these materials (N-doped RGO).

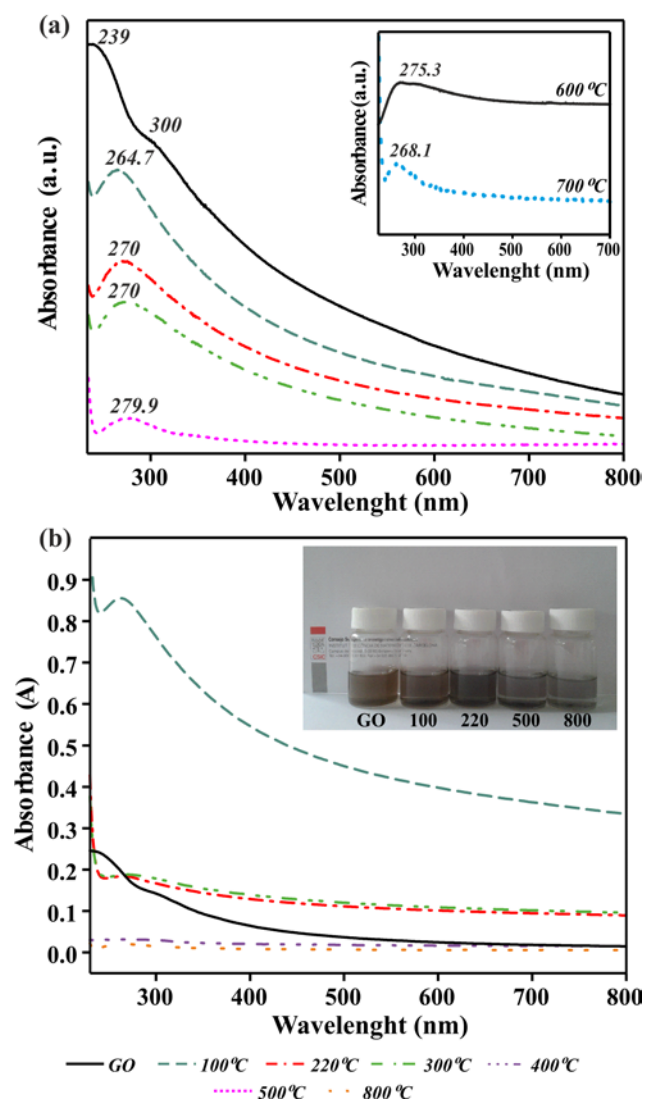


Figure 6. UV-Vis spectra of GO and NH_3 treated samples (a) after dispersion and (b) dispersion-centrifugation in water:ethanol (1:1).

Figure 7(a) presents the XPS general survey scans of graphene oxide before and after NH₃ treatment at 100 °C, 220 °C, 500 °C and 800 °C. As expected, the GO spectrum shows the signals of carbon and oxygen at binding energies of about 284 eV (C1s) and 530 eV (O1s). After the ammonolysis treatment, one additional peak becomes clearly visible corresponding to the N1s (binding energy ca. 400 eV). Thus confirming the presence of N in all the treated samples. For ease of comparison all the spectra are normalized to the intensity of the C1s peak (the C1s XPS region is presented in Figure S1). A continuous decrease in the relative amount of oxygen with respect to carbon is observed when increasing the temperature of the treatment; from 30.8 at. % of oxygen in GO down to 2.3 at. % of O already at 600 °C (Table 2). This highlights the efficiency of ammonia as reducing agent for the synthesis of reduced graphene oxide. No significant changes in the at. % of O are observed above 600 °C. To our best knowledge the level of oxygen achieved in this work (600-800 °C NH₃ treatments) accounts for the most reduced samples of graphene oxide (RGO) reported to date with temperatures up to 1000 °C. When RGO is prepared under an inert Ar atmosphere at 800 °C, the level of oxygen is about 5.4 at. % (Table 2). Similar values are obtained under reducing H₂ atmospheres even at higher temperatures (1100 °C; 2.7-9.2 at. % O)[18, 20] or in the presence of N-doping conditions (ca. 3 at. % O).[39, 40] This stresses the role of NH₃ not only as nitrating source but also for the removal of oxygen-bearing functionalities.

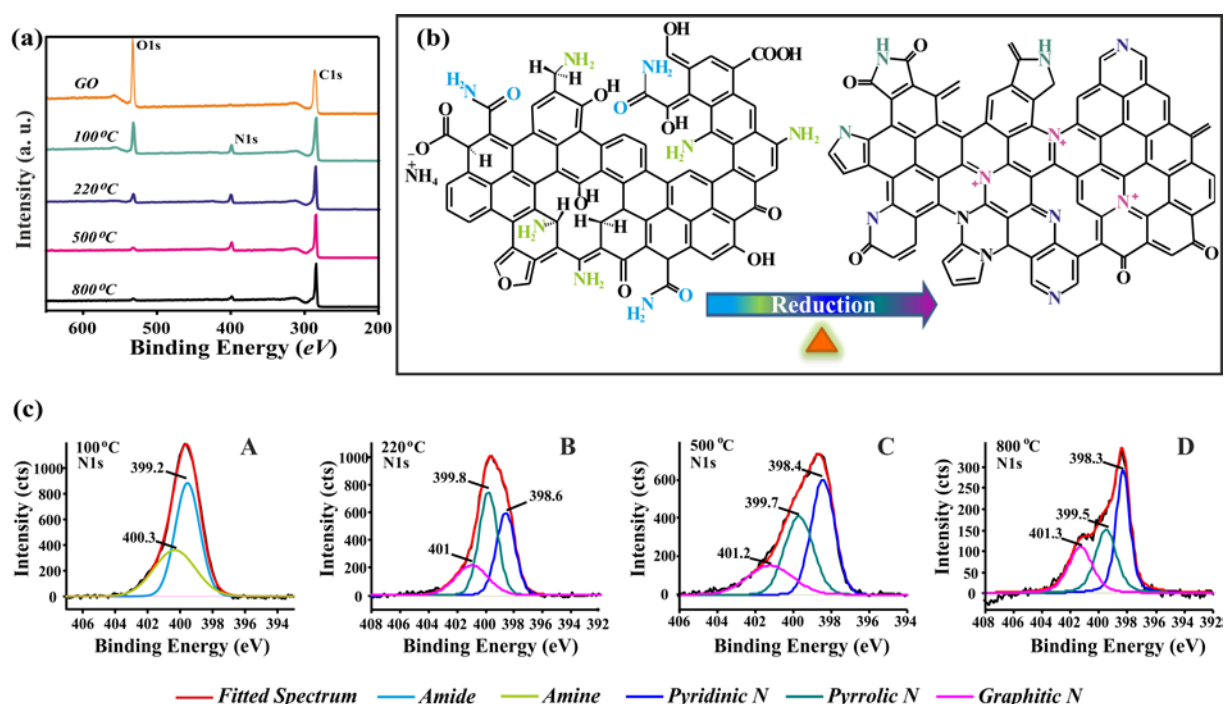


Figure 7. (a) XPS general survey scan of samples, (b) schematic representation of the nitrogen species introduced into the graphene lattice by the ammonia treatment and (c) high resolution N1s XPS spectra of NH₃ treated GO at (A) 100 °C, (B) 220 °C, (C) 500 °C and (D) 800 °C.

The high resolution N1s spectra show marked differences in the distribution of N species in the ammonia treated GO at different temperatures (Figure 7). The sample prepared at 100 °C (c-A) presents two well differentiated peaks that can be assigned to amide (399.2 eV) and amine (400.3 eV) functionalities. The binding energies of these peaks are in good agreement with the report of Gabriel et al., where well defined organic molecules, namely 4,5-ethylenedithio4',5' di(methylcarbamoyl)-tetrathiafulvalene and 4-aminothiophenol were employed to respectively define the peak position of amide and amine functionalities.[41]

Although both signals could also arise from the presence of pyridinic and pyrrolic N, all the analyses performed so far complementary confirm the presence of aliphatic nitrogenated species. When GO is treated under ammonia at 220 °C, a new peak appears at higher binding energy (ca. 401 eV) corresponding to graphitic N (quaternary N).[4] As per TGA, the elimination of oxidized functional groups begins to be important at this temperature. This suggests that a fraction of the N atoms are already integrated into the graphene lattice (N-doping) by substitution of the eliminated carbon atoms. A schematic representation of the different nitrogen functionalities that can be present in the prepared samples is presented in Figure 7. The scheme also illustrates that the environment of the nitrogen atoms and the level of reduction is temperature dependent.

The 5.2 % relative increase in the pyrrolic/amine signal (399.8 eV) and the strong decrease of O=C groups (42.3 %) in the sample treated at 220 °C, with respect to the 100 °C sample (Table S2), might account for the formation of N-bearing 5-membered rings resulting from the reaction of ammonia with dicarbonylic species (Scheme S2).[38] At 500 °C a decrease of intensity of the peak at 399.8 eV is observed and it is thought to only arise from pyrrolic N. Taking into consideration the previously performed analyses, the presence of aliphatic functionalities is not expected at this temperature of synthesis. Higher temperature treatments (800 °C) favour the formation of graphitic N (401.3 eV).

The high resolution O1s XPS also presents significant differences in the distribution of the O species (Figure 8). Therefore, the temperature employed for the treatments not only determines the degree of reduction (elimination of oxygen leading to RGO) but also allows tuning the nature of the oxygen-bearing functionalities in the resulting material. Three different signals assigned to O-C=O (ca. 531 eV), O=C (ca. 532 eV) and O-C (ca. 534 eV) are present in GO and NH₃ treated samples.[19] Comparison between the 100 °C and 500 °C samples reveals a significant decrease of both O=C (88.7 %) and O-C=O groups (87.7 %) in the latter (Table 2). The removal of O-C groups (26.3 %) takes place in a lesser extent, since these moieties present a higher stability against thermal oxidation.[34] An additional 35.7% loss of O-C functionalities is observed upon increasing the temperature of treatment to 800 °C. To get further insights on the impact that the ammonia treatment has on the distribution of oxygen bearing functionalities, the O1s spectra of GO annealed at 500 °C and 800 °C under Ar is included in Figure 8(h-i). Noticeably, a new peak around 535 eV appears which increases with the treatment temperature. This new peak, not present in the ammonia treated GO, can be assigned to aromatic derivatives resulting from condensation reactions of phenolic groups, previously observed in oxidized carbonaceous materials.[42] Some authors have also reported the presence of phenolic groups in GO by analysis of the C1s peak, overlapping with the alcohol/ether signal (ca. 285.4 eV).[43, 44]

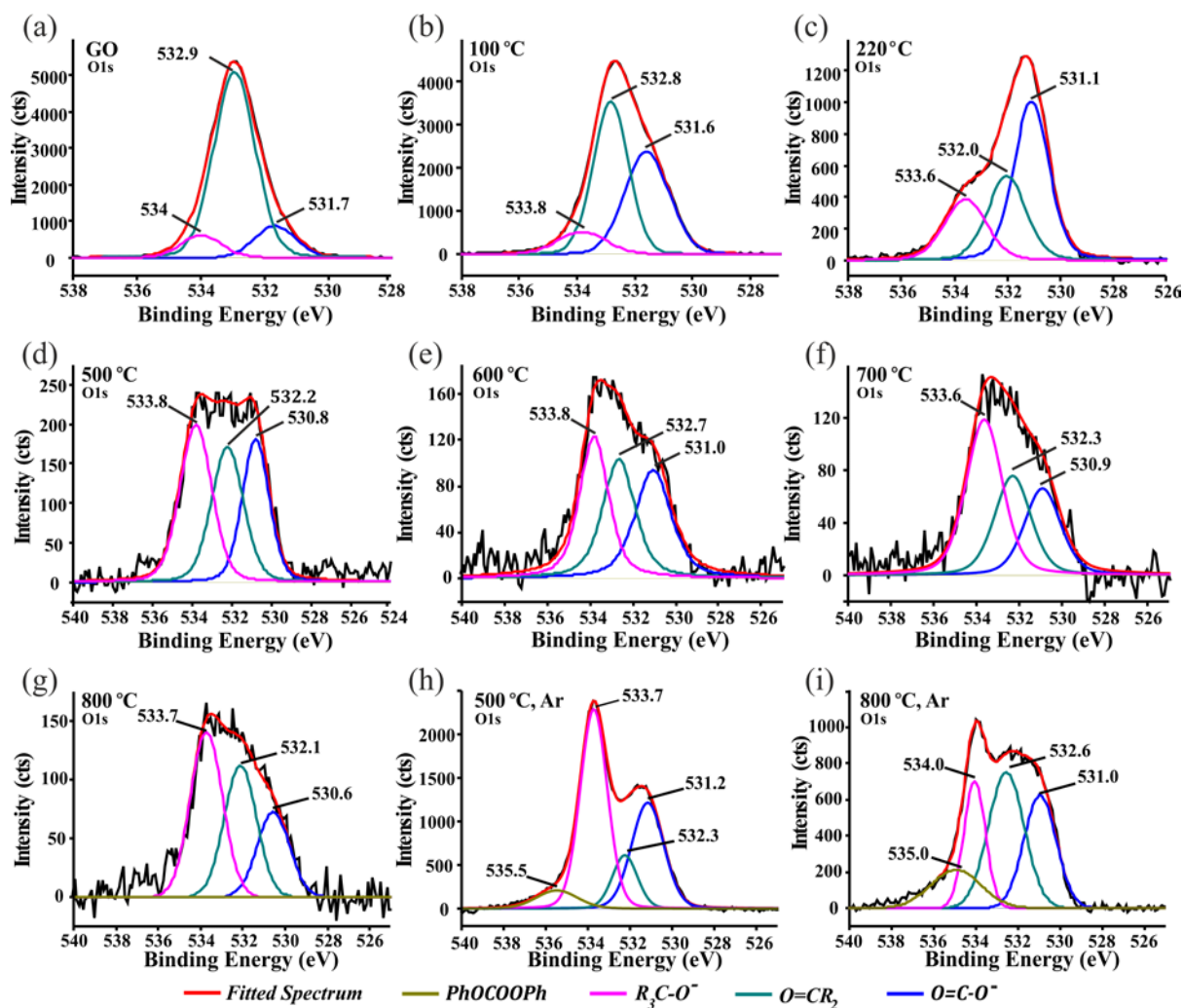


Figure 8. High resolution O1s spectra of (a) GO, (b-g) NH_3 treated GO (100 °C to 800 °C) and (h-i) Ar treated GO (500 °C and 800 °C).

Table 2. N, O and C content of GO, NH₃ treated GO (100 °C-800 °C) and Ar treated GO (500 °C, 800 °C) as determined by XPS analysis. (*) These at. % might also include contribution from aliphatic functionalities (amides or amines)

Sample	N content (at. %)					O content (at. %)				C content (at. %)
	Amide	Amine	Pyridinic N	Pyrrolic N	Graphitic N	O=C-O	O=C	O-C	PhOCOOPh	
GO	--	--	--	--	--	3.92	24.0	2.9	--	68.5
Total	0.7					30.8				
100 °C	4.6	3.2	--	--	--	8.1	9.7	1.9	--	72.5
Total	7.8					19.7				
220 °C	--	--	3.9*	4.7*	2.4	4.4	2.5	2	--	80.1
Total	11.0					8.9				
500 °C	--	--	4.5	3.7	2.1	1	1.1	1.4	--	86.2
Total	10.3					3.5				
600 °C	--	--	4.0	3.6	2.4	0.7	0.8	0.8	--	87.7
Total	10.0					2.3				
700 °C	--	--	2.9	2.6	2.2	0.5	0.6	0.9	--	90.3
Total	7.7					2				
800 °C	--	--	2.3	1.8	1.6	0.5	0.7	0.9	--	92.2
Total	5.7					2.1				
500 °C,Ar	--	--	--	--	--	3.9	1.5	6.1	0.9	87.0
Total	0.6					12.4				
800 °C Ar	--	--	--	--	--	1.5	2.0	1.1	0.8	94.1
Total	0.5					5.4				

Raman spectroscopy is a useful tool frequently employed to detect variations in the honeycomb carbon lattice.[45] To complete the present study, Raman spectra of the ammonia treated (100 °C-800 °C) and Ar reduced GO (800 °C) samples were recorded (Figure S2). As previously reported,[46] a down shift in the position of the G-band is observed by nitrogen doping of the graphene lattice, from 1600 cm⁻¹ (RGO) down to 1590.8 cm⁻¹ (N-doped RGO) - both samples being treated at 800 °C-. Furthermore, in agreement with the report of Cho et al.[47] an increase in the relative intensity of the D-band (I_D/I_G) is also observed after the ammonia treatment ($I_D/I_G = 1.10$ for N-doped RGO at 800 °C; $I_D/I_G = 0.95$ for RGO at 800 °C). The low temperature ammonia treated samples (100 °C-400°C) present a continuous increase of the I_D/I_G ratio when increasing the temperature of treatment (Fig. S2c). However, although all the N-doped samples (500 °C-800 °C) present similar I_D/I_G ratios, the opposite trend seems to take place.

4. Conclusions

To conclude, the nature of nitrogen in N-containing RGO has been tuned by thermal treatment of GO under ammonia. Low temperature treatments result in the formation of amine and amide N-bearing functionalities. The gas phase modification of GO to form amine and amide moieties is actually of interest by itself. Not only the use of gas phase treatments to modify GO has been less explored than solution treatments but also the attachment of amine/amide moieties to graphene has been barely investigated. The amount of these aliphatic functionalities is progressively reduced on increasing the temperature of ammonolysis leading to N-doped RGO. It is also worth noticing that highly reduced samples (ca. 2 % at. O) are obtained under mild conditions of treatment (600 °C) compared to previously reported protocols (1100 °C). Special care must be taken to determine the type of nitrogen present in graphene-related materials. XPS being the most widely employed technique to identify functional groups cannot discern between amine-pyrrole and amide-pyridine functionalities. We have shown that a proper assessment of the N-containing moieties cannot only rely on a

single XPS analysis but rather requires the use of complementary techniques. Towards this end we have employed not only FTIR and UV-Vis, but also benefit from TGA, contact angle measurements and the degree of dispersability of the prepared samples, which have not been previously investigated for the assessment of the N-bearing moieties in graphene.

Acknowledgements

We acknowledge financial support from MINECO (grants ACI2009-0861 and MAT2011-24757, Spain) and Department of Science and Technology (DST, India). This work has been carried out under the Materials Science PhD program of the Universitat Autònoma de Barcelona (UAB). The XPS data was acquired at the Laboratorio de Microscopías Avanzadas (LMA) - Instituto de Nanociencia de Aragón (INA), and EA in the Centres Científics i Tecnològics - Universitat de Barcelona, both in Spain.

References

- [1] Vashist SK, Luong JHT. Recent advances in electrochemical biosensing schemes using graphene and graphene-based nanocomposites. *Carbon*. 2015;84(0):519-50.
- [2] Geim AK. Graphene: status and prospects. *Science*. 2009;324(5934):1530-4.
- [3] Rao CN, Sood AK, Subrahmanyam KS, Govindaraj A. Graphene: the new two-dimensional nanomaterial. *Angew Chem Int Ed Engl*. 2009;48(42):7752-77.
- [4] Wang H, Maiyalagan T, Wang X. Review on Recent Progress in Nitrogen-Doped Graphene: Synthesis, Characterization, and Its Potential Applications. *ACS Catal*. 2012;2(5):781-94.
- [5] Tang Q, Zhou Z, Chen Z. Graphene-related nanomaterials: tuning properties by functionalization. *Nanoscale*. 2013;5(11):4541-83.
- [6] Liu H, Liu Y, Zhu D. Chemical doping of graphene. *J Mater Chem* 2011;21(10):3335-45.
- [7] Park M, Lee T, Kim B-S. Covalent functionalization based heteroatom doped graphene nanosheet as a metal-free electrocatalyst for oxygen reduction reaction. *Nanoscale*. 2013;5(24):12255-60.
- [8] Lin Z, Waller GH, Liu Y, Liu M, Wong C-p. Simple preparation of nanoporous few-layer nitrogen-doped graphene for use as an efficient electrocatalyst for oxygen reduction and oxygen evolution reactions. *Carbon*. 2013;53(0):130-6.
- [9] Gopalakrishnan K, Govindaraj A, Rao CNR. Extraordinary supercapacitor performance of heavily nitrogenated graphene oxide obtained by microwave synthesis. *J Mater Chem A*. 2013;1(26):7563-5.
- [10] Li S-M, Yang S-Y, Wang Y-S, Lien C-H, Tien H-W, Hsiao S-T, et al. Controllable synthesis of nitrogen-doped graphene and its effect on the simultaneous electrochemical determination of ascorbic acid, dopamine, and uric acid. *Carbon*. 2013;59(0):418-29.
- [11] Liu Y, Feng Q, Tang N, Wan X, Liu F, Lv L, et al. Increased magnetization of reduced graphene oxide by nitrogen-doping. *Carbon*. 2013;60(0):549-51.
- [12] Purceno AD, Machado BF, Teixeira APC, Medeiros TV, Benyounes A, Beausoleil J, et al. Magnetic amphiphilic hybrid carbon nanotubes containing N-doped and undoped sections: powerful tensioactive nanostructures. *Nanoscale*. 2015;7(1):294-300.
- [13] Sandoval S, Kumar N, Sundaresan A, Rao CNR, Fuertes A, Tobias G. Enhanced Thermal Oxidation Stability of Reduced Graphene Oxide by Nitrogen Doping. *Chemistry – A European Journal*. 2014;20(38):11999-2003.
- [14] Xin Y, Liu J-g, Jie X, Liu W, Liu F, Yin Y, et al. Preparation and electrochemical characterization of nitrogen doped graphene by microwave as supporting materials for fuel cell catalysts. *Electrochim Acta*. 2012;60(0):354-8.
- [15] Xiong B, Zhou Y, O'Hayre R, Shao Z. Facile single-step ammonia heat-treatment and quenching process for the synthesis of improved Pt/N-graphene catalysts. *Appl Surf Sci*. 2013;266(0):433-9.
- [16] Wei D, Liu Y, Wang Y, Zhang H, Huang L, Yu G. Synthesis of N-Doped Graphene by Chemical Vapor Deposition and Its Electrical Properties. *Nano Lett*. 2009;9(5):1752-8.
- [17] Panchakarla LS, Subrahmanyam KS, Saha SK, Govindaraj A, Krishnamurthy HR, Waghmare UV, et al. Synthesis, Structure, and Properties of Boron- and Nitrogen-Doped Graphene. *Adv Mater*. 2009;21(46):4726-30.
- [18] Li X, Wang H, Robinson JT, Sanchez H, Diankov G, Dai H. Simultaneous Nitrogen Doping and Reduction of Graphene Oxide. *J Am Chem Soc*. 2009;131(43):15939-44.
- [19] Wang Y, Shao Y, Matson DW, Li J, Lin Y. Nitrogen-Doped Graphene and Its Application in Electrochemical Biosensing. *ACS Nano*. 2010;4(4):1790-8.
- [20] Jiang B, Tian C, Wang L, Sun L, Chen C, Nong X, et al. Highly concentrated, stable nitrogen-doped graphene for supercapacitors: Simultaneous doping and reduction. *Appl Surf Sci*. 2012;258(8):3438-43.

- [21] Long D, Li W, Ling L, Miyawaki J, Mochida I, Yoon SH. Preparation of nitrogen-doped graphene sheets by a combined chemical and hydrothermal reduction of graphene oxide. *Langmuir*. 2010;26(20):16096-102.
- [22] Shi Z, Kutana A, Yakobson BI. How Much N-Doping Can Graphene Sustain? *The Journal of Physical Chemistry Letters*. 2015;6(1):106-12.
- [23] Wang X, Hou Z, Ikeda T, Oshima M, Kakimoto M-a, Terakura K. Theoretical Characterization of X-ray Absorption, Emission, and Photoelectron Spectra of Nitrogen Doped along Graphene Edges. *J Phys Chem A*. 2012;117(3):579-89.
- [24] Tobias G, Shao L, Salzmann CG, Huh Y, Green MLH. Purification and Opening of Carbon Nanotubes Using Steam. *J Phys Chem B*. 2006;110(45):22318-22.
- [25] Bianco A, Cheng H-M, Enoki T, Gogotsi Y, Hurt RH, Koratkar N, et al. All in the graphene family – A recommended nomenclature for two-dimensional carbon materials. *Carbon*. 2013;65(0):1-6.
- [26] White AH, Melville W. The Decomposition of Ammonia at High Temperatures. *J Am Chem Soc*. 1905;27(4):373-86.
- [27] Meyer JC, Geim AK, Katsnelson MI, Novoselov KS, Obergfell D, Roth S, et al. On the roughness of single- and bi-layer graphene membranes. *Solid State Commun*. 2007;143(1–2):101-9.
- [28] Hontoria-Lucas C, López-Peinado AJ, López-González JdD, Rojas-Cervantes ML, Martín-Aranda RM. Study of oxygen-containing groups in a series of graphite oxides: Physical and chemical characterization. *Carbon*. 1995;33(11):1585-92.
- [29] Shao L, Tobias G, Salzmann CG, Ballesteros B, Hong SY, Crossley A, et al. Removal of amorphous carbon for the efficient sidewall functionalisation of single-walled carbon nanotubes. *Chem Commun* 2007(47):5090-2.
- [30] Dyer J. *Applications of Absorption Spectroscopy of Organic Compounds*. New Jersey: Prentice Hall; 1965.
- [31] Kim UJ, Furtado CA, Liu X, Chen G, Eklund PC. Raman and IR Spectroscopy of Chemically Processed Single-Walled Carbon Nanotubes. *J Am Chem Soc*. 2005;127(44):15437-45.
- [32] Atkins P, Paula Jd. *Physical Chemistry for the Life Sciences*. Second ed. Oxford, U. K.: Oxford University Press.; 2009.
- [33] Pérez del Pino Á, György E, Cabana L, Ballesteros B, Tobias G. Deposition of functionalized single wall carbon nanotubes through matrix assisted pulsed laser evaporation. *Carbon*. 2012;50(12):4450-8.
- [34] Romanos GE, Likodimos V, Marques RRN, Steriotis TA, Papageorgiou SK, Faria JL, et al. Controlling and Quantifying Oxygen Functionalities on Hydrothermally and Thermally Treated Single-Wall Carbon Nanotubes. *J Phys Chem C*. 2011;115(17):8534-46.
- [35] Eda G, Chhowalla M. Chemically Derived Graphene Oxide: Towards Large-Area Thin-Film Electronics and Optoelectronics. *Adv Mater*. 2010;22(22):2392-415.
- [36] Zhou X, Shi T, Wu J, Zhou H. Facet-exposed anatase-phase TiO₂ nanotube hybrid reduced graphene oxide composite: Synthesis, characterization and application in photocatalytic degradation. *Appl Surf Sci*. 2013;287(0):359-68.
- [37] Hassan FM, Chabot V, Li J, Kim BK, Ricardez-Sandoval L, Yu A. Pyrrolic-structure enriched nitrogen doped graphene for highly efficient next generation supercapacitors. *J Mater Chem A*. 2013;1(8):2904-12.
- [38] Roberts J. *Basic Principles of Organic Chemistry*. New York: W. A. Benjamin, Inc.; 1965.
- [39] Jin J, Fu X, Liu Q, Liu Y, Wei Z, Niu K, et al. Identifying the Active Site in Nitrogen-Doped Graphene for the VO²⁺/VO²⁺ Redox Reaction. *ACS Nano*. 2013;7(6):4764-73.
- [40] Kumar NA, Nolan H, McEvoy N, Rezvani E, Doyle RL, Lyons MEG, et al. Plasma-assisted simultaneous reduction and nitrogen doping of graphene oxide nanosheets. *J Mater Chem A*. 2013;1(14):4431-5.
- [41] Gabriel G, Sauthier G, Fraxedas J, Moreno-Mañas M, Martínez MT, Miravittles C, et al. Preparation and characterisation of single-walled carbon nanotubes functionalised with amines. *Carbon*. 2006;44(10):1891-7.
- [42] Cha C, Shin SR, Annabi N, Dokmeci MR, Khademhosseini A. Carbon-Based Nanomaterials: Multifunctional Materials for Biomedical Engineering. *ACS Nano*. 2013;7(4):2891-7.
- [43] Desimoni E, Casella GI, Salvi AM. XPS/XAES study of carbon fibres during thermal annealing under UHV conditions. *Carbon*. 1992;30(4):521-6.
- [44] Szabó T, Berkesi O, Forgó P, Josepovits K, Sanakis Y, Petridis D, et al. Evolution of Surface Functional Groups in a Series of Progressively Oxidized Graphite Oxides. *Chem Mater*. 2006;18(11):2740-9.
- [45] Zhao L, He R, Rim KT, Schiros T, Kim KS, Zhou H, et al. Visualizing Individual Nitrogen Dopants in Monolayer Graphene. *Science*. 2011;333(6045):999-1003.
- [46] Lv R, Li Q, Botello-Méndez AR, Hayashi T, Wang B, Berkdemir A, et al. Nitrogen-doped graphene: beyond single substitution and enhanced molecular sensing. *Sci Rep*. 2012;2.
- [47] Park SH, Chae J, Cho M-H, Kim JH, Yoo K-H, Cho SW, et al. High concentration of nitrogen doped into graphene using N₂ plasma with an aluminum oxide buffer layer. *Journal of Materials Chemistry C*. 2014;2(5):933-9.